Extended Ethidium Bromide Analogue as a Triple Helix Intercalator: Synthesis, Photophysical Properties and Nucleic Acids Binding

Victor K. Tam, Qi Liu, and Yitzhak Tor*

Department of Chemistry and Biochemistry, University of California, San Diego,

La Jolla, CA 92093-0358

Supporting Information

General Considerations. All chemicals were obtained from commercial suppliers and used without further purification unless otherwise specified. Anhydrous solvents were used where noted and obtained using a two-column purification system (Glasscontour Systems, Irvine, CA). Analytical thin-layer chromatography was performed on pre-coated silica gel aluminum-backed plates (Kieselgel 60 F254, E. Merck & Co., Germany). Flash chromatography was performed using silica gel (230-400 mesh) from E.M. Science or Silicycle. NMR solvents were purchased from Cambridge Isotope Laboratories (Andover, MA). All NMR spectra were recorded on a Varian Mercury 400MHz instrument with chemical shifts reported relative to residual deuterated solvent peaks. Chemical shifts (δ) are reported in parts per million (ppm); multiplicities are indicated by s (singlet), d (doublet), t (triplet), q (quartet), dd (doublet of doublet), or m (multiplet); coupling constants (*J*) are reported in Hertz. Mass spectra were recorded at the UCSD Mass Spectrometry Facility, utilizing either a LCQDECA (Finnigan) ESI with a quadrupole ion trap or a MAT900XL (ThermoFinnigan) FAB double focusing mass spectrometer.

Spectrophotometric Experiments.

UV-Visible Experiments. UV-Visible experiments were carried out at ambient temperature in a quartz micro cell with a path length of 1.0 cm (Hellma GmbH & Co KG, Müllheim, Germany) on a Hewlett Packard 8452A diode array spectrometer. Both ethidium bromide and the 8-extended analogue samples were measured at 1.0×10^{-5} M (1% MeOH) in the appropriate spectroscopic grade solvent.

Thermal UV-Visible Denaturing Experiments. Thermal denaturing profiles were obtained using a Beckman Coulter DU® 640 Spectrophotometer with a high performance temperature controller and micro auto six holder. All hybridizations and UV melting experiments were carried out in 2.0×10^{-2} M PIPES (pH 7.0), 1.0×10^{-3} M EDTA, and 2.0×10^{-1} M NaCl. DNA oligonucleotides dA_{19} and dT_{19} were obtained from Integrated DNA Technologies (Coralville, IA) and purified using denaturing PAGE. Concentrations of oligonucleotide stocks were determined by using molar extinction coefficients 231,400 M^{-1} cm^{-1} for dA_{19} and 154,500 M^{-1} cm^{-1} for dT_{19} at 260 nm. RNA oligonucleotides rA_{19} and rU_{19} were obtained from Dharmacon RNA Technologies (Lafayette, CO) and purified using denaturing PAGE. Concentrations of oligonucleotide stocks were determined by using molar extinction coefficients 231,400 M^{-1} cm^{-1} for rA_{19} and 184,500 M^{-1} cm^{-1} for rU_{19} at 260 nm.

DNA double stranded (T·A) and triple-stranded (T·A·T) samples were prepared by mixing a 1:1 or 1:2 molar ratio of dA_{19} and dT_{19}, respectively. RNA triple-stranded (U·A·U) samples were prepared in a similar fashion with r_A and rU_{19}. The concentration of ligand (10.0 μM) and total triple helix (1.0 μM) was maintained as a ratio of [ligand]:[triple helix] = 10.0. Samples were pre-formed by heating to 90 °C for 3 min then slowly cooled to room temperature over one hour. After reaching room temperature, the samples were further cooled in an ice bath for 20 min to reach temperatures favorable for triple helix formation. At the beginning of each thermal denaturing experiment, all samples were held at 5 °C for 30 min in order to stabilize preformed triple helixes. Samples were placed in a stoppered 1.0 cm path length cell and a background spectra (buffer) was subtracted from each sample. All melting curves were obtained upon increasing the temperature from 5 °C to 80 °C at a rate of 1.0 °C min and absorbance

measurements at 260 nm were performed every minute. Beckman Coulter software (provided with T_m Analysis Accessory for DU® Series 600 Spectrometers) determined the duplex melting temperatures by calculating the first derivative of the melting profile.

Fluorescence Spectroscopy. Steady State fluorescence experiments were carried out at ambient temperature (unless otherwise noted) in a micro fluorescence cell with a path length of 1.0 cm (Hellma GmH & Co KG, Mullenheim, Germany) on a Perkin Elmer LS 50B luminescence spectrometer. Both ethidium bromide and the 8-extended analogue samples were measured at 5.0×10^{-6} M (0.5% MeOH) in the appropriate spectroscopic grade solvent (excitation slit = 7.0 nm, emission slit = 7.0 nm, scan speed = 300 nm/min, spectra averaged over three scans).

S.1: Synthetic Procedures & Characterization Data (^{1}H-NMR, ^{13}C-NMR, MS)

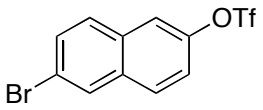

6-bromonaphthalen-2-yl trifluoromethanesulfonate (3): 6-bromo-2-naphthol (6 g, 27 mmol) was dissolved in anhydrous CH_2Cl_2 (100 mL) in a 500 mL round-bottom flask. Anhydrous pyridine (20 mL) was added, and the solution was cooled to –40ºC. Trifluoromethanesulphonic anhydride (Tf_2O) (7.62 g, 27 mmol) was added drop wise by addition funnel. The reaction was gradually warmed to r.t. and stirred for an additional 2 h. TLC (CH_2Cl_2, R_f 0.9) showed the reaction was complete. The reaction was concentrated to dryness and then partitioned between saturated NH_4Cl and CH_2Cl_2. The organic layer was dried over Na_2SO_4 and purified by silica flash chromatography (100% CH_2Cl_2) to yield a clear oil (9.42 g, 98% yield). ^{1}H NMR (400 MHz, DMSO-d_6): δ 8.30 (d, *J* = 2.0 Hz, 1H), 8.14 (d, *J* = 2.4 Hz, 1H), 8.08 (d, *J* = 9.2 Hz, 1H), 8.00 (d, *J* = 9.2 Hz, 1H), 7.74–7.14 (dd, *J1* = 8.8 Hz, *J2* = 2.0 Hz, 1H), 7.63–7.60 (dd, *J1* = 8.8 Hz, *J2* = 2.8 Hz, 1H). ^{13}C NMR (100 MHz, DMSO-d_6): δ 146.9, 133.2 131.5, 130.7, 130.2 (2), 129.8, 120.8, 120.7, 119.5. MS (EI) calculated for $C_{11}H_6BrF_3O_3S$ $[M^-]^+$ 353.92, found 354.0.

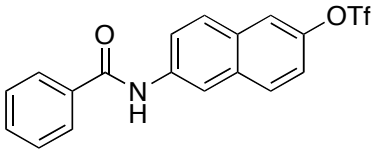

6-benzamidonaphthalen-2-yl trifluoromethanesulfonate (4): CuI (413 mg, 2.17 mmol), *N*,*N'*-dimethylethylenediamine (385 mg, 4.35 mmol), and K_2CO_3 (6 g, 43.5 mmol) were added to dry toluene (100 mL) in a 250 mL round-bottomed flask under argon. The mixture was stirred for 10 min to form the pre-catalyst, then compound **3** (7.7 g, 21.7 mmol) and benzamide (3.95 g, 32.63 mmol) were added under argon. The reaction was heated to 100ºC in a sealed flask for 48 h. TLC (CH_2Cl_2, R_f 0.4) showed the reaction was complete. After cooling the reaction to r.t., the crude was passed through a plug of silica gel (200 mL) and washed with copious amounts CH_2Cl_2, then concentrated to dryness to afford an off-white solid (8.3 g, 96% yield). ^{1}H NMR (400 MHz, DMSO-d_6): δ 10.57 (s, 1H), 8.60 (d, J = 1.2 Hz, 1H), 8.06 (t, J = 8.4 Hz, 3H), 8.01 (d, J = 7.2 Hz, 2H), 7.96–7.93 (dd, J_1 = 8.8 Hz, J_2 = 1.6 Hz, 1H), 7.64–7.54 (m, 4H). ^{13}C NMR (100 MHz, DMSO-d_6): δ 166.0, 145.9, 138.2, 134.7, 132.6, 131.8, 130.4, 129.6, 128.6, 128.4, 127.7, 122.5, 120.0, 119.1, 116.2. MS (ESI) calculated for $C_{18}H_{12}F_3NO_4S$ $[M+H]^+$ 396.04, found 395.94.

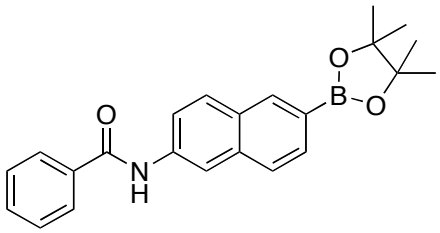

***N*-(6-(4,4,5,5-tetramethyl-1,3,2-dioxaborolan-2-yl)naphthalene-2-yl)benzamide (5)**: $Pd(dppf)Cl_2$ (52 mg, 0.063 mmol) and compound **4** (500 mg, 1.26 mmol) were dissolved in dry dioxane (10 mL) in a 100 mL round-bottom flask under argon. Et_3N (507 mg, 5 mmol), 4,4,5,5-tetramethyl-[1,3,2]dioxaborolane (644 mg, 5 mmol) were subsequently added. The reaction was stirred at 95 ºC under argon for 18 hours. TLC (CH_2Cl_2, R_f 0.3) showed the reaction was done. After cooling the reaction to r.t., it was passed through a plug of silica gel (50 mL), washed with CH_2Cl_2, and then concentrated to dryness. The crude was purified by flash column chromatography (60-100% CH_2Cl_2/hexanes) to yield a solid (306 mg, 65% yield) and triflate-reduced side product (53 mg, 17% yield). ^{1}H NMR (400 MHz, DMSO-d_6): δ 10.50 (s, 1H), 8.47 (d, J = 1.2 Hz, 1H), 8.26 (s, 1H), 8.01-7.98 (m, 3H), 7.86–7.81 (m, 2H), 7.68 (d, J = 8.0 Hz, 1H), 7.61-7.53 (m, 3H), 1.33 (s, 12H). ^{13}C NMR (100 MHz, DMSO-d_6): δ 165.9, 138.0, 135.6, 135.0, 134.9, 131.7, 130.5, 129.3, 129.1, 128.4, 127.7, 126.7, 121.0, 116.1, 83.7, 24.7. MS (ESI) calculated for $C_{23}H_{24}BNO_3$ $[M+H]^+$ 374.18, found 374.14.

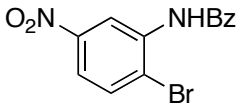

***N*-(2-bromo-5-nitrophenyl)benzamide (6)**: 2-bromo-5-nitroaniline (1.5 g, 6.9 mmol) and Et_3N (1.9 mL) were added to dry CH_2Cl_2 (15 mL) at 0ºC. Benzoyl chloride (1.46 g, 10.42 mmol) was added slowly. The reaction was refluxed for 12 h. TLC (80% CH_2Cl_2/hexanes, R_f 0.6) showed the reaction was complete. The reaction was partitioned between H_2O and CH_2Cl_2. The organic phase was dried over Na_2SO_4 and concentrated to dryness to afford a yellow solid (1.5 g, 70% yield). ^{1}H NMR (400 MHz, DMSO-d_6): δ 10.32 (s, 1H), 8.48 (s, 1H), 8.04-8.01 (m, 4H), 7.66-7.55 (m, 3H). ^{13}C NMR (100 MHz, DMSO-d_6): δ 165.3, 146.7, 137.5, 133.8, 133.2, 132.0, 128.4, 127.6, 127.2, 122.1, 121.7. MS (ESI) calculated for $C_{13}H_9BrN_4O_3$ $[M+H]^+$ 320.98, found 320.95.

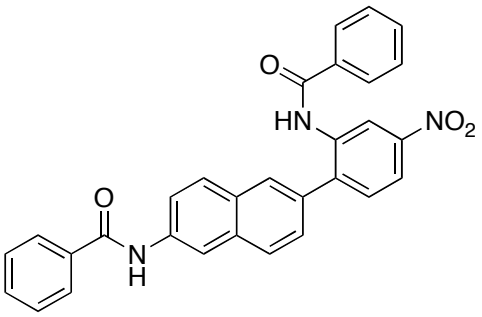

***N*-(6-(*N*-(3-nitrophenyl)benzamide))naphthalene-2-yl)benzamide (7)**: Compound **6** (100 mg, 0.3 mmol) and compound **5** (117 mg, 0.3 mmol) were added to DMF (3 mL) and 1M aqueous Na_2CO_3 (1.5 mL) and flushed with argon. $Pd(dppf)Cl_2$ (12.7 mg, 0.015 mmol) was added under argon and the reaction was stirred at 80ºC for 16 h. TLC (80% CH_2Cl_2/hexane, R_f 0.3) showed the reaction was complete. After cooling the reaction to r.t., volatiles were removed under vacuum. The residue was dissolved in CH_2Cl_2 and passed through a plug of silica gel (40 mL), washed with copious amounts of CH_2Cl_2, and then concentrated to dryness. The product was purified by flash column chromatography (100% CH_2Cl_2) to yield a yellow solid (140 mg, 95% yield).

For larger scale reactions (932 mg, 2.5 mmol of boronic ester in this instance), the product can be isolated by precipitation. After removal of volatiles, the crude was washed with water (50 mL) and isolated by vacuum filtration. Purification of the product is aided by its insolubility in most solvents. Successive precipitation of the yellow solid in acetone removes most impurities. Any remaining product in the acetone mother liquor can be isolated by flash column chromatography. Yield: 828 mg (68%); yellow solid. ^{1}H NMR (400 MHz, DMSO-d_6): δ 10.50 (s, 1H), 10.22 (s, 1H), 8.55 (d, *J* = 2.0 Hz, 1H), 8.51 (s, 1H), 8.24–8.21 (dd, *J1* = 8.8 Hz, *J2* = 2.4 Hz, 1H), 8.06 (s, 1H), 8.01 (d, *J* = 7.6 Hz, 2H), 7.96–7.86 (m, 3H), 7.82–7.79 (m, 3H), 7.63–7.59 (m, 2H), 7.55–7.52 (m, 3H), 7.47–7.43 (m, 2H). ^{13}C NMR (100 MHz, DMSO-d6): δ

165.9, 165.8, 146.6., 143.6, 137.6, 136.2, 134.8, 134.0, 133.6, 132.9, 131.8, 131.7 (2), 129.8, 128.6, 128.4 (3), 127.7, 127.6 (2), 126.6, 122.0, 121.4, 121.0, 116.2. MS (ESI) calculated for $C_{30}H_{21}N_3O_4$ $[M+H]^+$ 488.16, found 488.03.

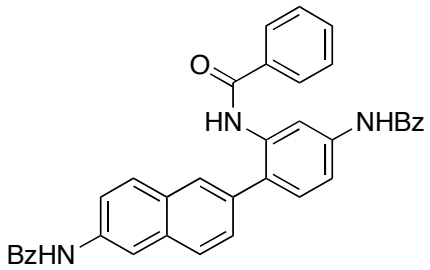

***N*-((6-(2,4-dibenzamide))naphthalene-2-yl)-benzamide (9)**: Compound **7** (175 mg, 3 mmol) was dissolved in EtOH (5 mL) in a 50 mL round-bottom flask. Hydrazine (80%, 0.1 mL) and 10% Pd/C (30 mg) were added under argon. The reaction was stirred at 65 ºC under H_2 (1 atm, balloon) for 4 h. TLC (5% MeOH/CH_2Cl_2, R_f 0.5) showed the reaction was complete. The reaction was cooled to room temperature and passed through a plug of Celite 500 (3 cm), washing with copious amount of MeOH. The filtrate was concentrated to dryness and briefly dried under high vacuum (< 1 torr). The crude was then dissolved in anhydrous DMF (5 mL) with Et_3N (0.5 mL) at 0ºC. Benzoyl chloride (0.078 mL, 0.72 mmol) was added to the flask. The reaction was stirred at r.t. for 12 h. TLC (5% MeOH/CH_2Cl_2, R_f 0.7) showed the reaction was complete. The reaction was filtered through Whatman #50 filter paper, and then partitioned between saturated $NaHCO_3$ and CH_2Cl_2. The organic phase was dried over Na_2SO_4 and concentrated to dryness. The product was purified by flash chromatography (2% MeOH/CH_2Cl_2) to yield a solid (171 mg, 85% yield). ^{1}H NMR (400 MHz, DMSO-d_6): δ 10.46 (s, 2H), 10.01 (s, 1H), 8.45 (s, 1H), 8.05-7.78 (m, 11H), 7.63-7.42 (m, 11H). ^{13}C NMR (100 MHz, DMSO-d6): δ 165.5, 165.4, 165.3, 138.6, 136.6, 135.1, 134.9, 134.7, 134.6, 134.3, 133.1, 131.2, 131.5, 131.4, 131.2, 130.3, 129.8, 128.3, 128.2, 128.1, 128.1, 127.5, 127.3, 127.2, 126.9, 126.8, 120.9, 119.6, 118.4, 116.0. MS (ESI) calculated for $C_{37}H_{27}N_3O_3$ $[M+H]^+$ 562.21, found 562.03.

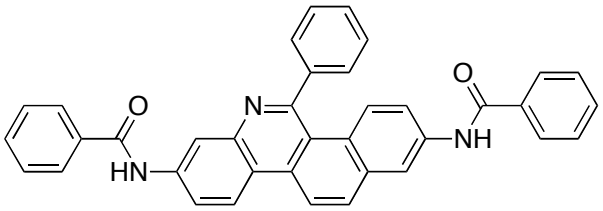

5-phenylbenzo[*i*]phenanthridine-2,8-dibenzyloxycarbamate (10): Compound **9** (260 mg, 0.46 mmol) was heated in $POCl_3$ (5 mL) at 100ºC for 18 hours. TLC (5% MeOH/CH_2Cl_2, R_f 0.3) showed the reaction was done. The reaction was cooled to 0ºC in an ice-water bath and $POCl_3$ was hydrolyzed with cold water. The solution was adjusted to pH 10 with concentrated NH_4OH. The resulting yellow precipitate (226 mg, 89% yield) was filtered through Whatman #50 filter paper and washed with water. ^{1}H NMR (400 MHz, DMSO-d_6): δ 10.70 (s, 1H), 10.52 (s, 1H), 8.88 (d, J = 9.2 Hz, 1H), 8.85 (d, J = 9.2 Hz, 1H), 8.72 (s, 1H), 8.63 (s, 1H), 8.31 (d, J = 8.8 Hz, 1H), 8.14 (d, J = 9.2 Hz, 1H), 8.04 (d, J = 7.6 Hz, 1H), 7.99 (d, J = 7.6 Hz, 1H), 7.65–7.51 (m, 13H). ^{13}C NMR (100 MHz, DMSO-d_6): δ 165.7, 165.5, 158.5, 139.8, 137.0, 134.6, 134.5, 133.1, 132.9, 131.5 (2), 128.7, 128.5, 128.2, 127.6, 127.5, 125.5, 123.4, 120.7, 120.6, 119.6, 119.4, 119.3, 117.7, 117.4. MS (ESI) calculated for $C_{37}H_{25}N_3O_2$ $[M+H]^+$ 544.20, found 544.38

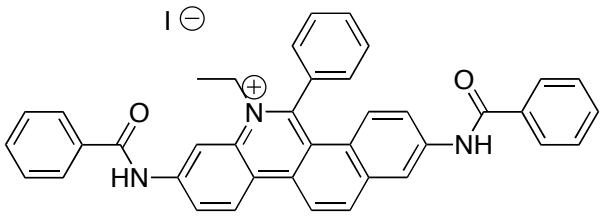

5-phenylbenzo[*i*]phenanthridine-2,8-dibenzyloxycarbamate *N*-ethyl iodide (11): Compound **10** (163 mg, 0.3 mmol) and EtI (1 mL) were refluxed in anhydrous DMF (5 mL) for 20 h. TLC (10% MeOH/CH_2Cl_2, R_f 0.4) showed the reaction was done. The reaction was concentrated to dryness and purified by flash chromatography (1-10% MeOH/CH_2Cl_2) to afford a red solid (147 mg, 71% yield). ^{1}H NMR (400 MHz, DMSO-d_6): δ 11.13 (s, 1H), 10.60 (s, 1H), 9.37 (d, J = 9.6 Hz, 1H), 9.25 (d, J = 1.2 Hz, 1H), 9.08 (d, J = 9.6 Hz, 1H), 8.74–8.72 (m, 2H), 8.53–8.51 (dd, J_1 = 9.2 Hz, J_2 = 1.2 Hz, 1H), 8.09–7.85 (m, 7H), 7.69–7.54 (m, 8H), 6.84 (d, J = 9.6 Hz, 1H), 4.75 (d, J = 6.8 Hz, 2H), 1.61 (t, J = 7.2 Hz, 3H). HRMS (FAB) calculated for $C_{39}H_{30}N_3O_2$ $[M]^+$ 572.2333, found 572.2348.

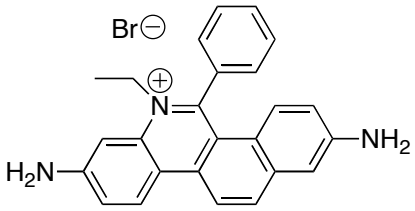

5-phenylbenzo[*i*]phenanthridine-2,8-diamine *N*-ethyl bromide (2): Compound **11** (200 mg, 0.28 mmol) was dissolved in 48% HBr (4 mL) and refluxed for 14 h. The reaction was concentrated to dryness and purified by flash chromatography (50 mL silica gel, 2-4% MeOH/CH_2Cl_2) to yield a red solid (100 mg, 80% yield). ^{1}H NMR (400 MHz, CD_3CN-d_3): δ 8.70 (d, J = 10.0 Hz, 1H), 8.50 (d, J = 9.2 Hz, 1H), 8.15 (d, J = 9.6 Hz, 1H), 7.82-7.74 (m, 3H), 7.56 (d, J = 6.8 Hz, 2H), 7.43 – 7.41 (dd, J_1 = 7.6 Hz, J_2 = 2.0 Hz, 2H), 7.08 (d, J = 2.8 Hz, 1H), 6.61 (d, J = 9.2 Hz, 1H), 6.55 – 6.52 (dd, J_1 = 9.6 Hz, J_2 = 2.8 Hz, 1H), 5.66 (s, 2H, NH_2), 4.67 (s, 2H, NH_2), 4.55 (q, J = 7.2 Hz, 2H), 1.46 (t, J = 6.8 Hz, 3H). HRMS (FAB) calculated for $C_{25}H_{22}N_3$ $[M]^+$ 364.1808, found 364.1808; UV (MeOH) λ_{max} = 512 nm (ε = 5200 cm^{-1} M^{-1}).

S.2: UV-Visible Spectra.

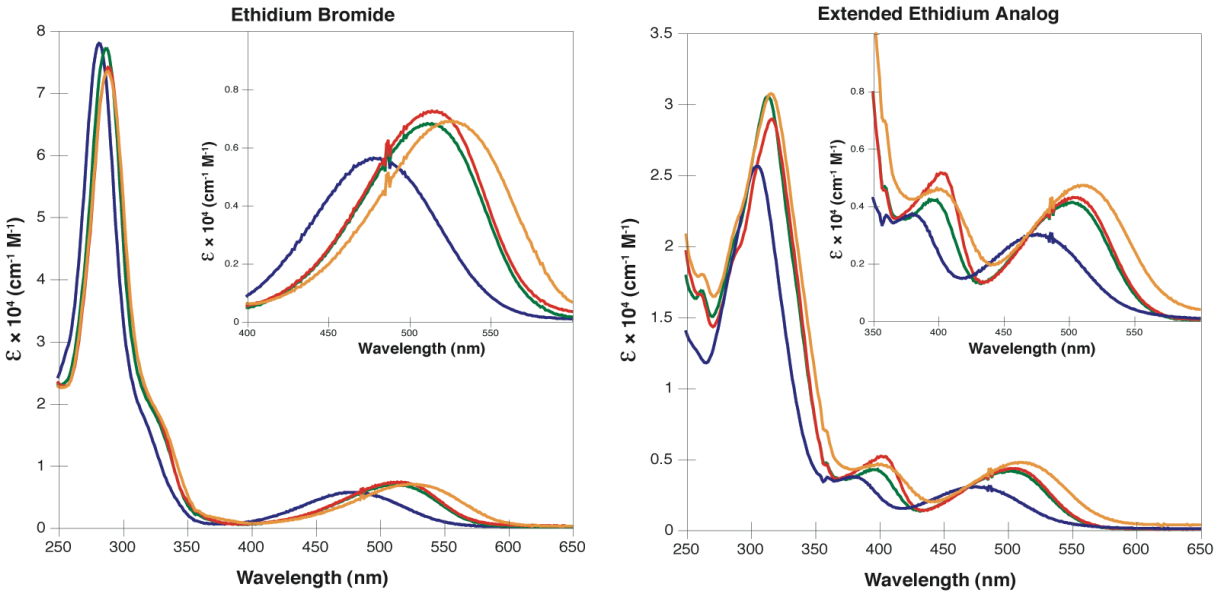

Figure S2.1. UV-Visible absorbance spectrum of ethidium bromide (left) and the extended ethidium analogue (right). In both spectra solvents are denoted as follows: CH_2Cl_2 (red); CH_3CN (green); MeOH (orange); and H_2O (blue). Equal concentrations (1.0×10^{-5} M) of compound are used in both spectra. For the extended ethidium analogue, a nonlinear dependence of absorbance on concentration is observed at concentrations near and above 1.0×10^{-5} M.

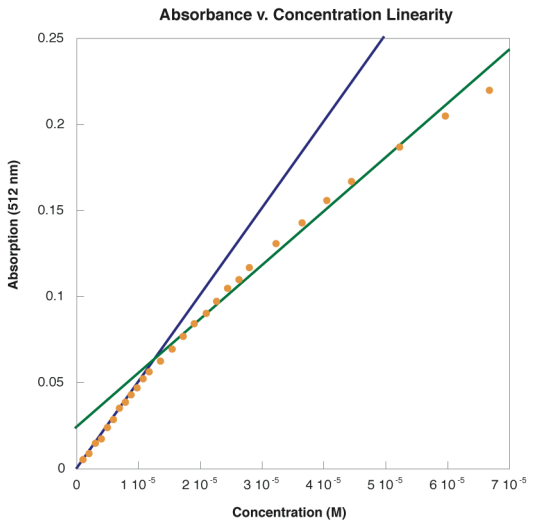

Figure S2.2. Relationship between absorbance and concentration for the extended ethidium analogue. At concentrations above 1.0×10^{-5} M, the dependence of absorbance on concentration deviates from linearity. The extinction coefficient was determined by a linear curve fit of absorbance versus concentration for extended ethidium concentrations between 1.0 to 10.0 μM.

S.3: Solvent-Dependent Steady State Fluorescence Emission Spectra

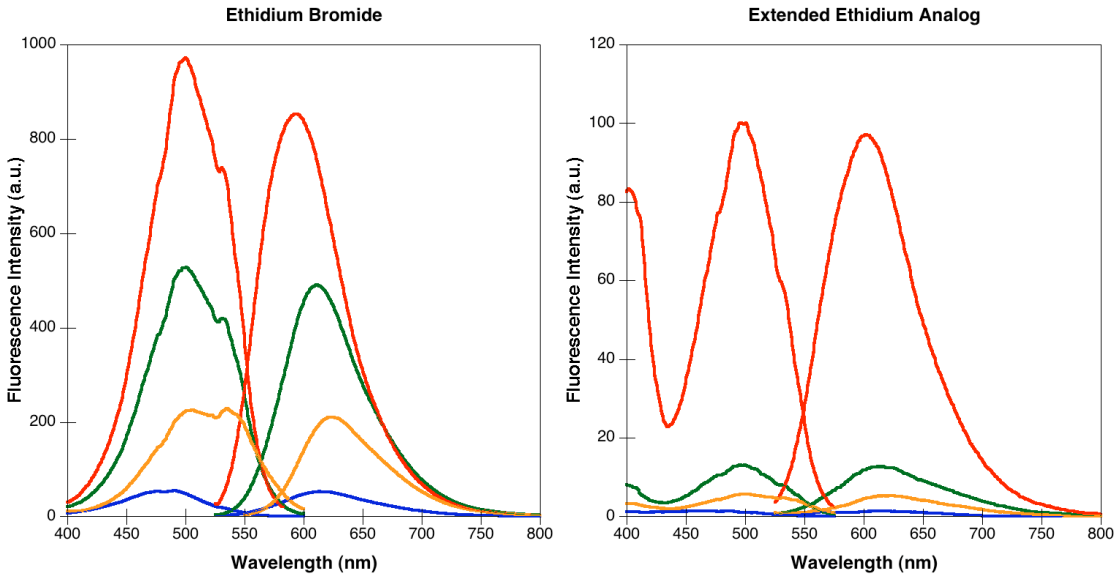

Figure S3.1. Emission and excitation spectra of ethidium bromide (left) and the extended ethidium analogue (right). In both spectra solvents are denoted as follows: CH_2Cl_2 (red); CH_3CN (green); MeOH (orange); and H_2O (blue). Spectra are plotted against different absolute fluorescence intensity but equal concentrations (5×10^{-6} M).

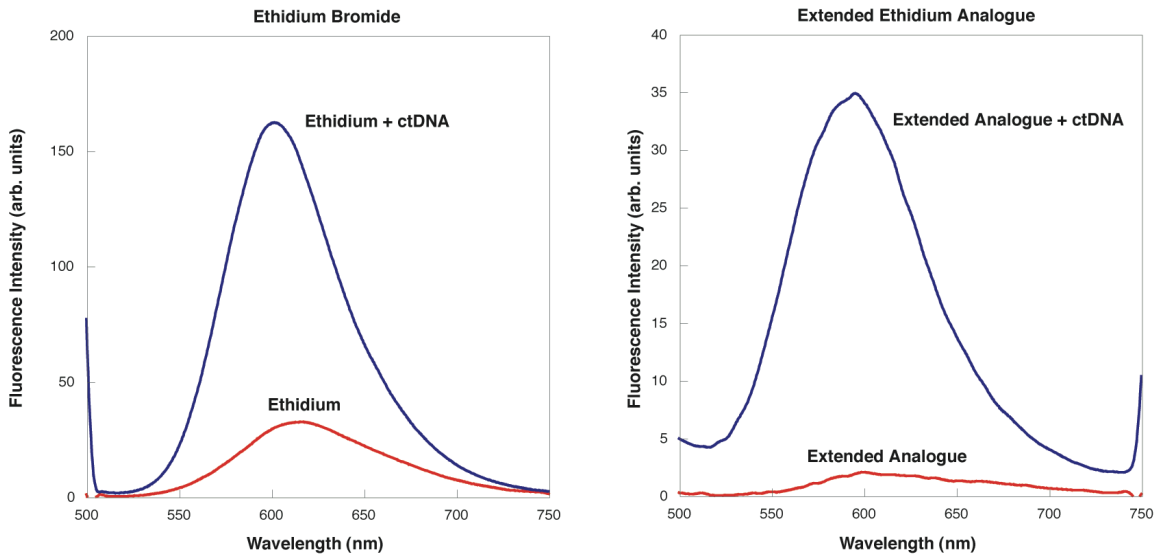

Figure S3.2. Fluorescence emission spectra of ethidium bromide (left) and the extended ethidium analogue (right) in the presence and absence of calf thymus DNA. Ligand samples were fully saturated with high concentrations of calf thymus DNA. Approximate fluorescence intensity increase upon binding to ctDNA is 3 to 4-fold for ethidium bromide and over 10-fold for the extended ethidium analogue.

Solvent Polarity Measurements.

The relationship between emission energy and microenvironment solvent polarity [$E_T(30)$] was determined for the 8-extended analogue. All emission spectra were determined at 5.0×10^{-6} M with 0.5% MeOH in four different solvents (water, methanol, acetonitrile and dichloromethane). Emission spectra were converted from wavelength (nm) to wave numbers (cm^{-1}). $E_T(30)$ values for each solvent were determined using Reichardt's salt (Reichardt, C. *Chem Rev.* **1994**, *94*, 2319–2358).

Relationship between Emission Energy and $E_T(30)$ Values.

Solvent	$E_T(30)$	Emission Energy of 8-extended analogue (cm^{-1})
Water	63.1	16,181
Methanol	55.0	16,051
Acetonitrile	48.1	16,340
Dichloromethane	44.0	16,611

S.4: Nucleic Acid Binding Fluorescence Studies

A sonicated solution of calf thymus (CT) DNA was purchased from Gibco BRL. Poly r(A)·r(U) was purchased from Sigma-Aldrich and poly d(A), poly d(T), poly r(A), and poly r(U) were purchased from Amersham Bioscience. Stock solutions were made in 1 × TE and quantified according to the following extinction coefficients in 50 mM sodium phosphate (pH 7.5) buffer at the stated wavelengths:

Nucleic Acid polymer	Extinction coefficient
calf thymus DNA	13,100 cm^{-1} M^{-1} per base pair (260 nm)
poly r(A)·r(U)	14,280 cm^{-1} M^{-1} per base pair (260 nm)
poly d(A)	8,600 cm^{-1} M^{-1} per base pair (257 nm)
poly d(T)	8,700 cm^{-1} M^{-1} per base pair (265 nm)
poly r(A)	9,900 cm^{-1} M^{-1} per base pair (260 nm)
poly r(U)	9,300 cm^{-1} M^{-1} per base pair (260 nm)

Buffer conditions.

All fluorescence titrations were conducted at ambient temperature in a "physiological" buffer containing 30 mM HEPES (pH 7.4), KCl (100 mM), Na_2HPO_4 (10 mM), guanidinium hydrochloride (20 mM), $MgCl_2$ (2 mM), NaCl (20 mM), EDTA (0.5 mM), and Nonidet P-40 (0.001%).

Fluorescence Titrations.

In a Perkin Elmer LS-50B luminescence spectrometer, a dilute solution of ethidium bromide or 8-extended analogue (1.0 μM) in "physiological" buffer was excited at 479 nm or 389 nm,

respectively. The emission of each compound was monitored near 605 nm (excitation slits = 10 nm, emission slits = 20 nm, scan speed = 300 nm/min, averaged over three scans). Small volumes of highly concentrated nucleic acids were titrated, with a small increase in the final volume (≤10%) of the sample. Data analysis accounts for the small change in volume. Titrations with duplex nucleic acid polymers were performed at ambient temperature. Titrations with polymeric triple helices were conducted at 0 °C with a thermally jacketed cuvette holder. All triple helical samples were maintained at 0 °C during these titrations.

Fluorescence Titration Data Analysis.

The fractional change in emission intensity was taken as the fraction of ethidium or ethidium analogue bound (χ) and was used to calculate the concentration of free nucleic acid [NA] and concentration of bound analogue [$EtBr_{bound}$] at each concentration of nucleic acid [NA_{tot}] (total concentration). The calculated fractional saturation was fit to the following equation using Kaleidagraph to derive binding affinity (K_d) of ethidium and 8-extended analogue for each respective nucleic acid:

$$\chi_{bound} = \frac{[NA]^n}{[NA]^n + K_d}$$

where *n* is the Hill coefficient or degree of cooperativity associated with binding (in most cases n~1).

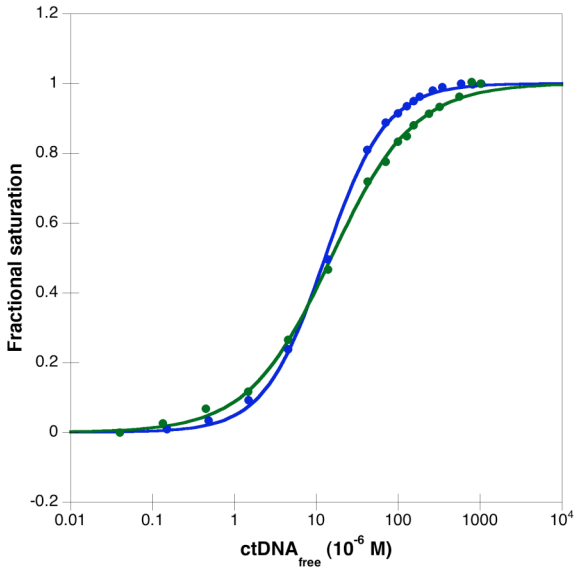

Figure S4.1 Binding isotherms of ethidium bromide (blue) and extended ethidium analogue (green) with calf thymus DNA.

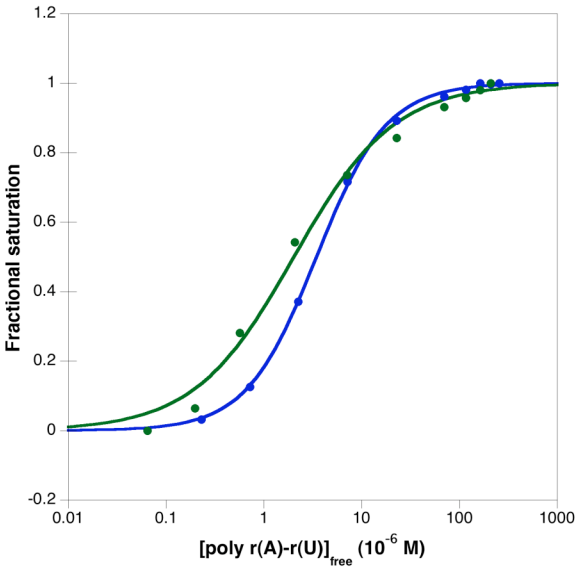

Figure S4.2 Binding isotherm of ethidium bromide (blue) and extended ethidium analogue (green) with poly r(A)·r(U).

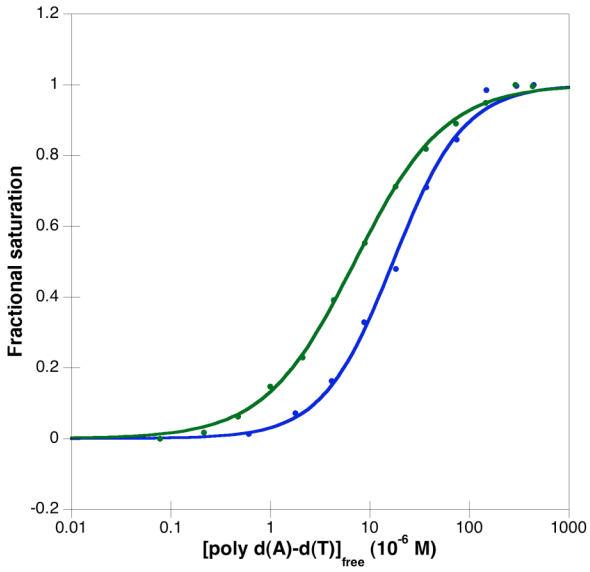

Figure S4.3 Binding isotherm of ethidium bromide (blue) and extended ethidium analogue (green) with poly d(A)·d(T).

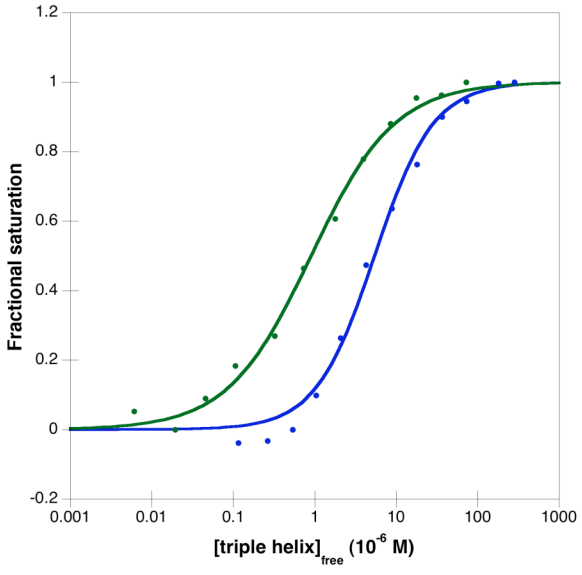

Figure S4.4 Binding isotherm of ethidium bromide (blue) and extended ethidium analogue (green) with triple helix poly d(T)·d(A)·d(T).

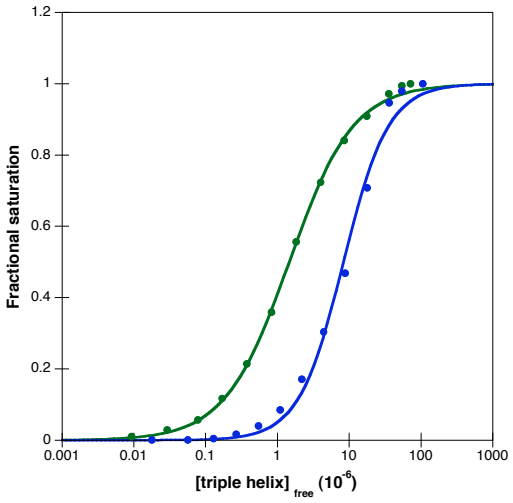

Figure S4.5 Binding isotherm of ethidium bromide (blue) and extended ethidium analogue (green) with triple helix poly r(U)·r(A)·r(U).

S.5 UV-Visible Thermal Melting Studies

The affinities of **1** and **2** to an RNA triple helix r(A)·r(U)·r(A) were determined and found to correlate well with previous studies reporting the destabilizing effect of **1** to induce duplex formation (see Le Pecq & Paoletti, *C. R. Acad. Sc. Paris* **1965**, *260*, 7033–7036). Although an equilibrium mixture of duplex and triplex RNA may exist during the fluorescence titration, Lehrman and Crothers report that in a 1:2 stoichiometric ratio of poly r(A) and poly r(U), respectively, this mixture binds **1** with a lower affinity than an RNA duplex of 1:1 poly r(A) and poly r(U) (see Lehrman & Crothers, *Nuc. Acids Res.* **1977**, *4*, 1381–1392). Thermal melting profiles also illustrate the destabilizing effect of **1** on the RNA triple helix by absence of the triplex-duplex transition, while the transition in the presence of **2** is still observable.

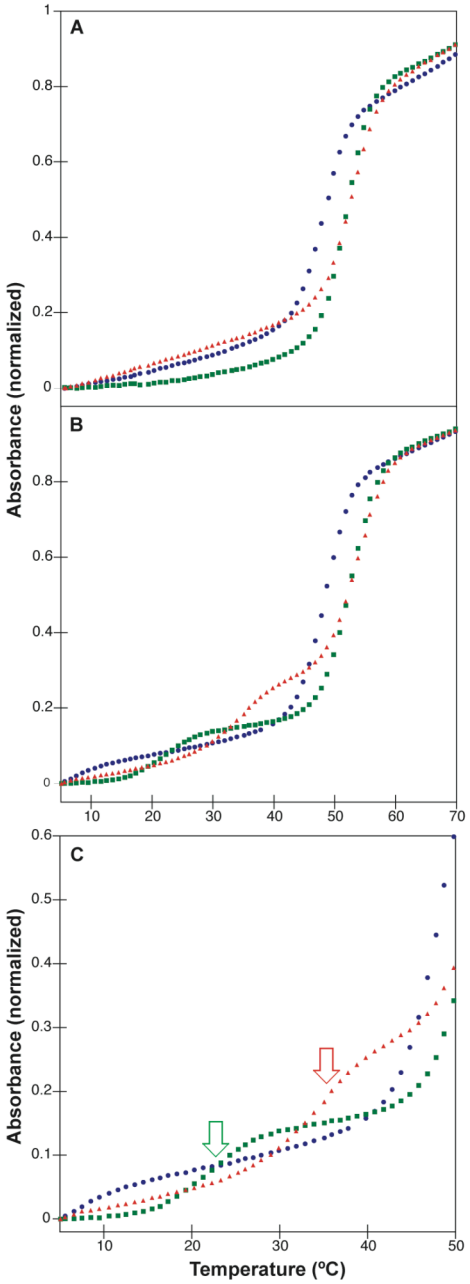

Figure S5.1 Thermal melting profiles for (A) $dA_{19}{\cdot}dT_{19}$ and (B) $dT_{19}{\cdot}dA_{19}{\cdot}dT_{19}$ with no ligand (●), ethidium bromide (■), and the extended ethidium analogue (▲). The $T_m(2\rightarrow1)$ transition for both duplex and triple helix studies were similar in the absence and presence of both ligands. (C) is an expansion of the triple helix melting profile of (B).

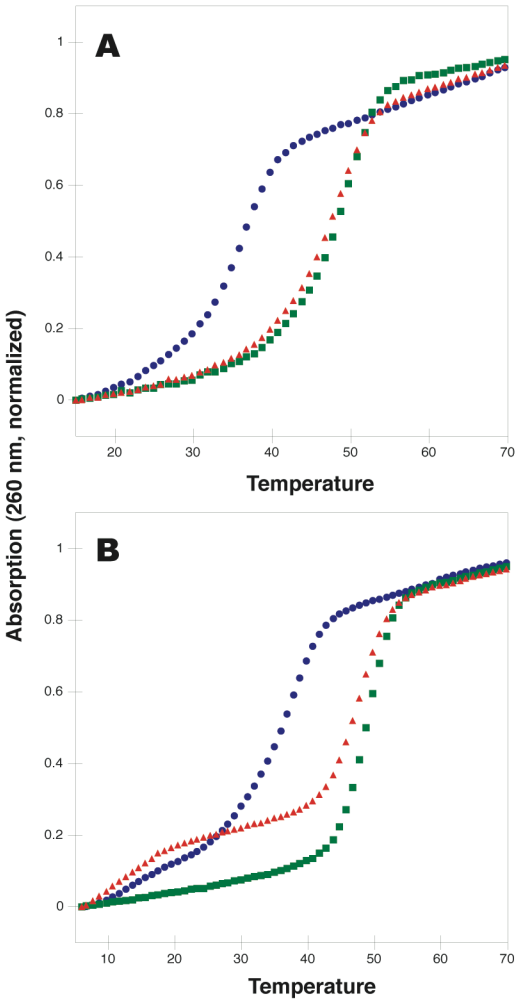

Figure S5.2 Thermal melting profiles for (A) $rA_{19}{\cdot}rU_{19}$ and (B) $rU_{19}{\cdot}rA_{19}{\cdot}rU_{19}$ with no ligand (●), ethidium bromide (■), and the extended ethidium analogue (▲). The $T_m(2\rightarrow1)$ transition for both duplex and triple helix studies were similar in the absence and presence of both ligands. The $T_m(3\rightarrow2)$ transition for ethidium bromide is not observed because of its destabilizing effect on the RNA triple helix

$dA_{19}·dT_{19}$		
	T_m(2→1)	**T_m(3→2)**
no ligand	48 ± 0.7 °C	---
ethidium bromide	52 ± 1.0 °C	---
extended ethidium bromide	53 ± 1.0 °C	---
$dT_{19}·dA_{19}·dT_{19}$		
no ligand	49 ± 0.1 °C	< 10 °C
ethidium bromide	53 ± 0.6 °C	24 ± 0.1 °C
extended ethidium bromide	54 ± 0.6 °C	37 ± 1.0 °C

$rU_{19}·rA_{19}·rU_{19}$		
	T_m(2→1)	**T_m(3→2)**
no ligand	37 ± 0.6 °C	13 ± 1.0 °C
ethidium bromide	49 ± 0.6 °C	none observed
extended ethidium bromide	49 ± 1.0 °C	14 ± 1.7 °C

Table S5.1 *(top)* Table of thermal melting points for the duplex $dA_{19}·dT_{19}$ and triple helix $dT_{19}·dA_{19}·dT_{19}$ in the presence and absence of ligands **1** or **2**. *(bottom)* Table of thermal melting points for the RNA triple helix $rU_{19}·rA_{19}·rU_{19}$ in the presence and absence of ligands **1** or **2**.